DOI: 10.1002/ejic.200600236

Molecular and Electronic Structures of Homoleptic Nickel and Cobalt Complexes with Non-Innocent Bulky Diimine Ligands Derived from Fluorinated 1,4-Diaza-1,3-butadiene (DAD) and Bis(arylimino)acenaphthene (BIAN)

Marat M. Khusniyarov,[a] Klaus Harms,[a] Olaf Burghaus,[a] and Jörg Sundermeyer*[a]

Dedicated to Professor Hansgeorg Schnöckel on the occasion of his 65th birthday

Keywords: EPR spectroscopy / Magnetochemistry / Non-innocent ligands / Nickel / Cobalt / X-ray diffraction

The diimine complexes with bulky fluorinated *N*-substituents $[Ni^{II}(^{F}DAD)_2]$ **1** and $[Co^{II}(^{F}DAD)_2]$ **2** [^{F}DAD = *N*,*N*′-bis-(pentafluorophenyl)-2,3-dimethyl-1,4-diaza-1,3-butadiene] as well as diimine complexes with extended π system $[Ni^{II}(^{F}BIAN)_2]$ **3** and $[Co^{I}(^{F}BIAN)_3]$ **4** (^{F}BIAN = bis[*N*-{3,5-bis(trifluoromethyl)phenyl}imino]acenaphthene) were synthesized. Compound **4** represents the first complex with three bis(imino)acenaphthene ligands synthesized so far. The molecular structures of the complexes **1**–**4** were determined by X-ray crystallography at 193 K. Complexes **1**, **2** and **3** comprise the divalent metal ions with pairs of radical monoanionic ligands, whereas **4** is best described as a cobalt(I) complex with two neutral $(^{F}BIAN)^0$ and one $(^{F}BIAN)^{1-}$ ligand in the radical monoanionic form. The electronic structures of the paramagnetic cobalt complexes **2** and **4** were investigated by SQUID measurements and X-band EPR spectroscopy. Both complexes possess a doublet ground state, with electron density located mostly in the metal d-orbitals. The doublet–quartet energy gap for **4** was established to be 159 cm^{-1}.

Introduction

Homoleptic complexes of substituted 1,4-**di**aza-1,3-buta-**d**iene (DAD) with late transition metals $[M(DAD)_2]$ are well know since the first publication of Balch and Holm in early 1966.[1] They synthesized the extremely oxygen-sensitive complex $[Ni\{Ph\text{-}DAD(Me)\}_2]$ and proposed the electronic structure as a Ni^{II} center with two radical monoanionic $(DAD)^{1-}$ ligands.

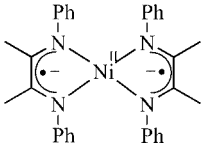

Nowadays, it is clearly established that the $(DAD)^0$ ligand possessing a low-lying antibonding π* orbital is able to accept one or two electrons giving open-shell monoanion $(DAD)^{1-}$ or closed-shell dianion $(DAD)^{2-}$, respectively. Thus, DAD along with related *o*-phenylenediamido ligands belong to the classical *N*,*N*′-coordinating non-innocent ligands.[2]

R'-DAD(R) :

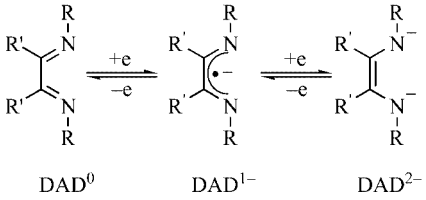

DAD^0 DAD^{1-} DAD^{2-}

The class of $[M(DAD)_2]$ complexes was expanded by the groups of tom Dieck (M = Fe,[3] Ni[4]) and von Walther (M = Fe,[5] Co,[5,6] Ni[7]). Later, several $[Ni(DAD)_2]$ complexes were characterized by single-crystal X-ray analysis.[8,9] In contradiction to the electronic model given by Balch and Holm all these complexes were formulated as zero-valent metal species with pairs of closed-shell $(DAD)^0$ ligands. At the same time closely related complexes derived from *o*-phenylenediamine $[Ni^{II}(sbqdi)_2]$[10] [sbqdi – **s**emi**b**enzo-**q**uinone**di**iminato(1–)] and diaminomaleonitrile $[Ni^{II}(sdisn)_2]$[11] [sdisn – **s**emi**di**imino**s**ucci**n**o**n**itrilo(1–)] are well known to consist of a divalent metal and a pair of monoanionic radical ligands.

[a] Fachbereich Chemie, Philipps-Universität Marburg, Hans-Meerwein-Straße, 35032 Marburg, Germany
Fax: +49-6421-28-28917
E-mail: jsu@chemie.uni-marburg.de

Supporting information for this article is available on the WWW under http://www.eurjic.org or from the author.

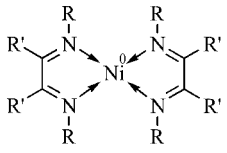

$[Ni(DAD)_2]$

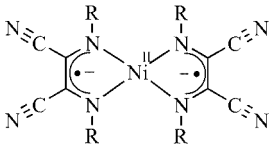

$[Ni(sdisn)_2]$

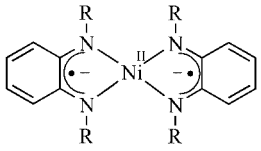

$[Ni(sbqdi)_2]$

Throughout this paper we carefully distinguish between formal[12] and spectroscopic (or physical)[13] oxidation states. The formal oxidation state of a metal ion in a given coordination compound is a non-measurable, physically meaningless, usually integral number that is derived by heterolytic removal of all ligands in their closed-shell electron configuration, whereas the spectroscopic oxidation state is derived from the actual electron configuration of the metal ion in a given ligand regime.

Complexes of late transition metals with redox active non-innocent ligands[2] are of particular interest with regard to their electronic structures. Since late transition metals can exist in several oxidation states, ambiguity of oxidation state determination may arise with transition metals coordinated to non-innocent ligands. Often spectroscopic (or physical) oxidation state of the non-innocent ligand can be elegantly determined using a high-quality single-crystal X-ray analysis, as different oxidation states of the ligand reveal different characteristic bond lengths.[14]

Following our studies on complexes of late transition metals containing non-innocent ligands[15] we report here the first structurally characterized $[Co(DAD)_2]$ complex along with its Ni analogue. Both molecular and electronic structures of them are being investigated by X-ray analysis, EPR spectroscopy, and variable-temperature magnetic susceptibility measurements.

Similar to DAD **b**is(aryl**i**mino)**ac**e**n**aphthene (BIAN)[16] owing to its non-innocent nature is known to form complexes in different ligand oxidation states.

Ar-BIAN:

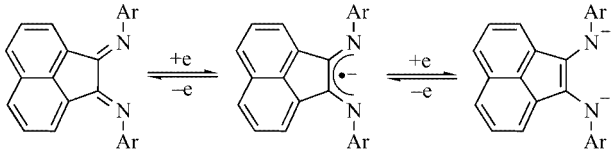

$BIAN^0$ $BIAN^{1-}$ $BIAN^{2-}$

Very recently, Fedushkin et al.[17] reported the first homoleptic complexes of the type $[M^{II}(BIAN)_2]$ (M = Mg, Ca). The molecular structure of $[Ca^{II}(dip\text{-}BIAN)_2]$ (dip = 2,6-diisopropylphenyl) was established and monoanionic nature of both ligands along with conventional oxidation state for calcium were established. To the best of our knowledge homoleptic complexes of the type $[M(BIAN)_2]$ with transition metals have been not isolated and structurally characterized so far. Therefore, the class of homoleptic DAD complexes has been further expanded by us to corresponding BIAN complexes. Molecular structures of BIAN complexes of nickel and cobalt are reported. The electronic structure of the paramagnetic cobalt complex is investigated in detail by means of EPR spectroscopy and variable-temperature magnetic susceptibility measurements.

Results and Discussion

Synthesis and Characterization of DAD Complexes

In order to synthesize complexes **1** and **2** we employed a variation of the well-known in situ reduction method.[7,8] Complexes **1** and **2** were obtained in moderate to high yields by complexation of anhydrous metal salts with two equivalents of the ligand in the presence of two equivalents of C_8K as a reducing agent. The target complexes are oxygen and moisture sensitive and should be handled and stored under strictly anaerobic conditions.

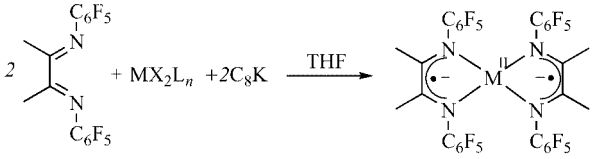

M = Ni, X = Br, L = DME, n = 1 $[Ni^{II}(^{F}DAD)_2]$ **1**

M = Co, X = Cl, n = 0 $[Co^{II}(^{F}DAD)_2]$ **2**

At room temperature complex **1** is diamagnetic in solution and shows three sharp multiplets in the ^{19}F NMR spectrum in the expected region –150 to –164 ppm vs. $CFCl_3$. It is interesting to note significant changes in the ^1H NMR spectrum accompanying the complexation. While in the free ligand the methyl group is observed at δ = 2.24 ppm, it is slightly broadened ($W_{1/2}$ = 6 Hz) and strongly high-field shifted in the complex and observed at δ = –1.98 ppm. The same observation was made by tom Dieck et al. for a series of $[Ni(DAD)_2]$ complexes.[8] We ascribe this unusual shift to residual paramagnetism of **1** derived from a low-lying triplet state populated at room temperature. The signal at δ = –1.98 ppm in the ^1H NMR spectrum of **1** is virtually temperature-independent, it is only slightly low-field shifted to –1.79 ppm by cooling the sample from 300 to 243 K.

Although a distorted tetrahedral environment of Ni^{II} (vide infra) results in high-spin complex (S_{Ni} = 1), the two radical ligands seem to couple antiferromagnetically with the metal giving ultimately a diamagnetic complex. Quenching of inherent paramagnetism of Ni^{II} in a distorted tetrahedral arrangement of two chelating radical ligands has recently been reported by Wieghardt et al.[18] EPR spectroscopy applied to **1** gave evidence for its diamagnetism. Complex **1** was X-band EPR silent in solution/frozen solution at temperatures 4–300 K.

Complex **2** is paramagnetic both in solid state and in solution, the effective magnetic moment, μ_{eff} = 3.26 (μ_B), was measured for the solid at room temperature. This value is close to the spin state S = 3/2, further investigation of the electronic structure of **2** is given below.

Crystal Structures of DAD Complexes

The molecular structure of **1** consists of two *N*,*N*′-chelating ^{F}DAD ligands coordinated to the metal center (Figure 1). Two ^{F}DAD ligands form a dihedral angle 55.28(9)° reflecting a twisted tetrahedral geometry at the metal center. The complex shows C_2 symmetry having twofold symmetry axis defined by Ni atom and the centroids of the diimine C–C bonds. Two metallacycles NiNCCN do not show any bend along NN′ axis, which would be the characteristic feature for doubly reduced DAD ligands.[19] In contrast they are essentially planar with maximum deviation of 0.031(2) Å from the best-fit planes defined by E_1 (Ni1N1C1C1′N1′) and E_2 (Ni1N2C3C3′N2′). The sum of angles at each nitrogen atom is close to 360° typical for planar sp^2-hybridized N-centers. Since the bond lengths in two diimines are the same within ±0.012 Å (3σ), two ligands have an identical oxidation state.

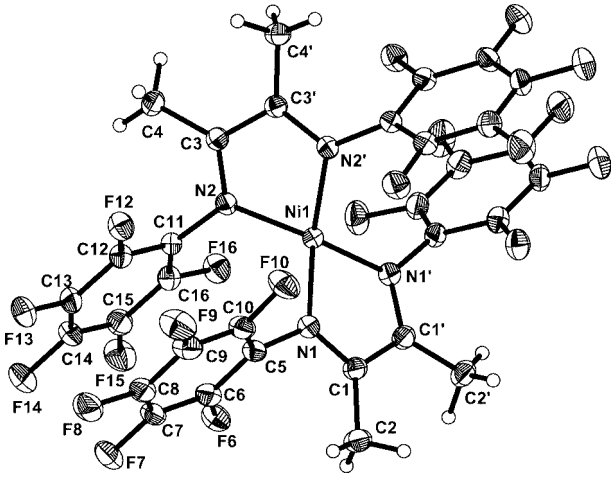

Figure 1. Molecular structure of **1**, thermal ellipsoids are drawn at 30% probability level.

The oxidation state of the ligands and consequently of the metal can be unambiguously assigned on the basis of the bond lengths analysis. In comparison of C–C and C–N bond lengths of diimine moieties in **1** (Table 1) with corresponding bond lengths in complexes, whose structures were determined accurately (Scheme 1), it is evident that both ligands in **1** are radical monoanions (^{F}DAD)$^{1-}$. The C–N bond length, on average 1.344(3) Å, along with the C–C bond of NCCN backbone, on average 1.413(5) Å, are in good agreement with the presence of an open-shell (^{F}DAD)$^{1-}$.[20] Since the complex possesses no extra charge, the physical (or spectroscopic)[13] oxidation state of Ni is +II (d^8 electronic configuration).

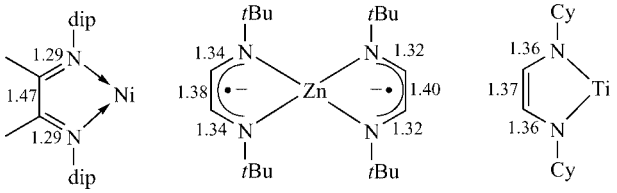

Scheme 1. Characteristic bond lengths for DAD ligand in different oxidation states: $(DAD)^0$ in $[Ni^{II}\{dip\text{-}DAD(Me)\}(CH_2SiMe_3)_2]$[38] (left), $(DAD)^{1-}$ in $[Zn^{II}\{t\text{Bu-}DAD(H)\}_2]$[20] (middle), and $(DAD)^{2-}$ in $[Ti^{IV}\{Cy\text{-}DAD(H)\}Cl_2(THF)_2]$[39] (right).

The molecular structures of several homoleptic complexes $[Ni(DAD)_2]$ were reported previously.[8,9] All of them were formulated as Ni^0 complexes containing a pair of closed-shell $(DAD)^0$ ligands. Taking into account the bond lengths of diimine moieties found in these complexes we suggest reformulation of their electronic structures. For example, the structure of $[Ni\{dmp\text{-}DAD(H)\}_2]$[8b] (dmp = 2,6-dimethylphenyl) reveals C–N bonds on av. 1.341(2) Å and C–C bonds of NCCN backbone on av. 1.374(2) Å. The bond length pattern observed in the former is in better agreement with the presence of the open-shell $(DAD)^{1-}$ rather than the closed-shell $(DAD)^0$. Having analyzed molecular structures of a series of reported $[Ni(DAD)_2]$ complexes we suggest new electronic structures for the following complexes: $[Ni^{II}\{Cy\text{-}DAD(H)\}^{1-}_2]$,[8a] $[Ni^{II}\{dmp\text{-}DAD(H)\}^{1-}_2]$,[8b] $[Ni^{II}\{t\text{Bu-}DAD(H)\}^{1-}_2]$,[9a] $[Ni^{II}\{dip\text{-}DAD(H)\}^{1-}_2]$.[9b]

Almost all related homoleptic *o*-phenylenediamine-derived complexes $[Ni^{II}(sbqdi)_2]$[10a,21] and the diaminomaleonitrile-derived $[Ni^{II}(sdisn)_2]$[11a] show strictly square-planar geometry, whereas **1** as well as $[Ni(DAD)_2]$ structurally characterized previously reveal twisted tetrahedral geometry. The dihedral angle formed by two diimine moieties varies from 44.5° in $[Ni\{dmp\text{-}DAD(H)\}_2]$[8b] to 88.95° in $[Ni\{t\text{Bu-}DAD(H)\}_2]$.[9a] The large deviation from a square-planar geometry observed in $[Ni(DAD)_2]$ complexes can be rationalized by steric repulsion of bulky *N*-substituents. In

Table 1. Selected bond lengths [Å] of complexes **1**–**4**.

$[Ni^{II}(^FDAD)_2]$ (**1**)		$[Co^{II}(^FDAD)_2]$ (**2**)		$[Ni^{II}(^FBIAN)_2]$ (**3**)		$[Co^{I}(^FBIAN)_3]$ (**4**)			
						I		**II**	
Ni1–N1	1.9173(18)	Co1–N1	1.932(3)	Ni1–N1	1.9399(15)	Co1–N1	2.144(2)	Co1–N3	2.125(2)
Ni1–N2	1.9165(17)	Co1–N2	1.931(3)	Ni1–N2	1.9370(15)	Co1–N2	2.119(2)		
C1–N1	1.340(3)	C7–N1	1.352(5)	C1–N1	1.333(2)	C1–N1	1.302(4)	C29–N3	1.331(3)
C3–N2	1.348(3)	C15–N2	1.357(5)	C2–N2	1.344(2)	C2–N2	1.304(3)		
C1–C1#	1.414(5)	C7–C7#	1.408(8)	C1–C2	1.427(3)	C1–C2	1.474(4)	C29–C29#	1.442(5)
C3–C3#	1.411(4)	C15–C15#	1.412(8)						

contrast, a series of $[Ni^{II}(sbqdi)_2]$ and $[Ni^{II}(sdisn)_2]$ complexes with small N–H substituents do not show any deviation from square-planar geometry, whereas $[Ni^{II}(sbqdi)_2]$ having bulky C_6F_5 groups attached to four nitrogen atoms does show tetrahedral distortion: the two planar ligands form dihedral angle of 53.7(1)°.[22]

The strong distortion from planarity in **1** is caused by interaction between the bulky C_6F_5 groups engaged in intramolecular C_6F_5–C_6F_5 stacking. The phenyl rings form dihedral angles in the range of 65.7(1)–67.3(1)° with corresponding diimine NCCN planes and are pairwise close to coplanar with an interplanar angle of 2.9(1)°. The smaller distance between C_6F_5 centroid and the least-squares plane of adjacent C_6F_5 ring is 3.23 Å. If we assume that complex **1** adopts a square-planar geometry without significant changes in bond lengths and angles, a simple geometrical consideration predicts that the coplanar C_6F_5 rings would be forced to a face-to-face distance of approximately 2.9 Å. Recently, by DFT calculations Lorenzo et al.[23] have shown that energy minimum for the gas-phase dimer $(C_6F_6)_2$ in face-to-face configuration is reached when the interplanar distance C_6F_6–C_6F_6 is 3.31–3.37 Å. Assuming that the energy minima for the pair C_6F_5–C_6F_5 in **1** and the calculated pair C_6F_6–C_6F_6 are reached at the close distances we expect strong repulsion between two pairs of C_6F_5 rings in the hypothetical square-planar complex **1**.

A tetrahedral distortion of the complex and synchronous rotation of the phenyl rings provide a relaxation of repulsive interaction and sufficient increase of the C_6F_5–C_6F_5 distances. The molecular structure of **1** reveals a slipped arrangement of two pairs of C_6F_5 rings. The interplanar C_6F_5–C_6F_5 distance found at 3.23 Å is in good agreement with distances 3.23 and 3.32 Å between C_6F_5 rings engaged in intramolecular stacking in the sandwich complex bis[η^5-1,2,4-tris(pentafluorophenyl)cyclopentadienyl]iron(II)[24] and with distances 3.20–3.28 Å in the series of complexes $[M(^{F}sbqdi)_2]$ [M = Co, Ni, Pd, Cu, ^{F}sbqdi – radical anion derived from doubly deprotonated *N*,*N*′-bis(pentafluorophenyl)-*o*-phenylenediamine].[22]

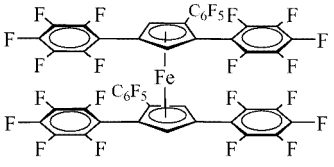

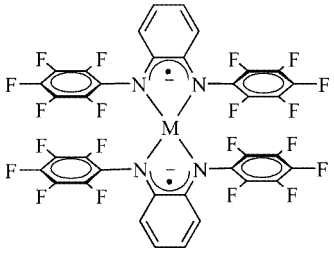

In conclusion, the twisted tetrahedral geometry of **1** is determined by repulsion forces between the two pairs of perfluorinated rings, which is a typical feature of four-coordinate Ni^{II} complexes with bulky ligands.

Although the synthesis of one homoleptic cobalt complex [Co{Ph-DAD(Ph)}$_2$] was reported earlier[5,6] up to now no structural information about $[Co(DAD)_2]$ complexes is available. The molecular structure of $[Co^{II}(^{F}DAD)_2]$ (**2**), which is isomorphous with **1**, is shown in Figure 2. The cobalt atom is located in a twisted tetrahedral environment of two chelating ^{F}DAD ligands, nearly planar diimine moieties form a dihedral angle of 58.0(2)°. The molecule is symmetrical having a C_2-axis defined by the cobalt atom and the centroids of the diimine C–C bonds. The five-membered metallacycles formed are essentially planar: the maximum deviation from the best-fit plane is 0.027(4) Å for both rings. The bond lengths and angles within the two ^{F}DAD moieties are the same within 3σ.

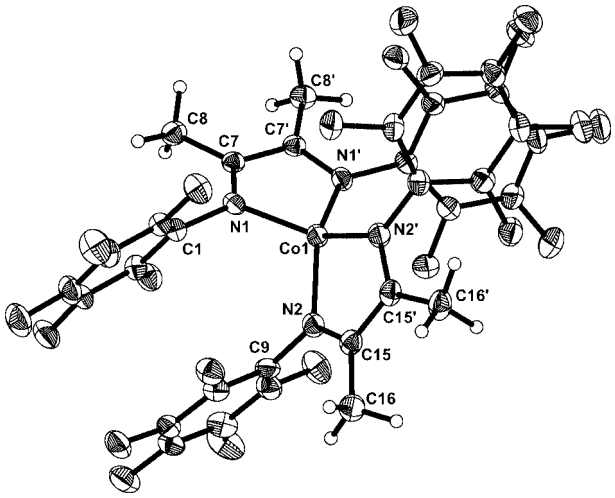

Figure 2. Molecular structure of **2** showing distorted tetrahedral geometry around the metal center; thermal ellipsoids are drawn at 30% probability level.

By comparison of the bond length pattern of the NCCN moieties in **2** with that of **1** it is found that ^{F}DAD ligands in both complexes are nearly similar. In complex **2** the C–N bond lengths on av. 1.355(5) Å along with the C–C bonds of the NCCN backbone on av. 1.410(8) Å are in good agreement with the presence of two radical monoanions $(^{F}DAD)^{1-}$. Taking into account that the complex is not charged we assign the cobalt oxidation state to be +II (d^7 electronic configuration).

Slight C–N bond lengthening of 0.011 Å along with negligibly small C–C bond shortening of 0.003 Å in NCCN backbone of **2** compared to **1** are ascribed to slightly higher population of π* orbitals of the ligands in **2**. Nearly coplanar C_6F_5 rings with a dihedral angle of 3.9(2)° display an interplanar distance close to that observed in **1**: the smaller distance between C_6F_5-centroid and the least-squares plane of adjacent C_6F_5 ring is 3.27 Å. Close interplanar distances C_6F_5–C_6F_5 observed for **1** and **2** confirm that the geometry of both complexes is governed by intramolecular C_6F_5–C_6F_5 interactions.

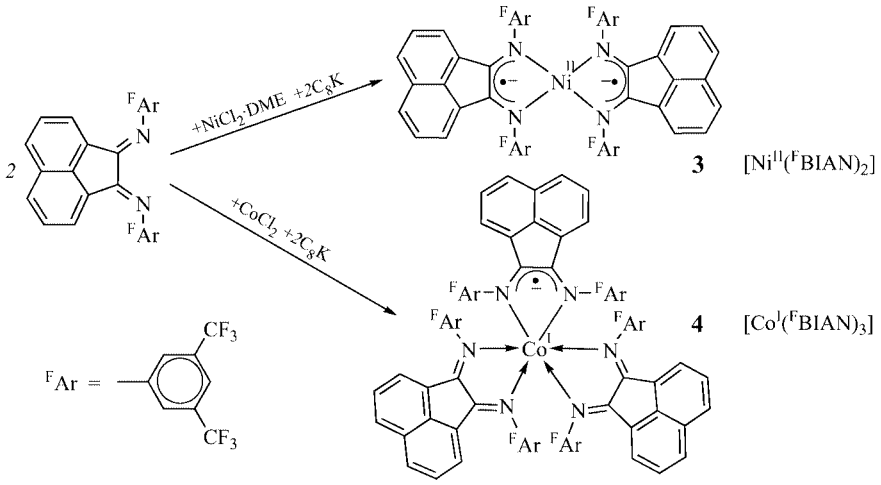

Synthesis and Characterization of BIAN Complexes

Complexes **3** and **4** were prepared by ligand reduction with C_8K in the presence of the metal salts as described before for ^{F}DAD complexes. Surprisingly, the reaction of 2 equiv. of the ligand with 1 equiv. of $CoCl_2$ gave neutral [Co(^{F}BIAN)$_3$] but not the expected [Co(^{F}BIAN)$_2$]. Subsequent reaction of $CoCl_2$ with 3 equiv. of ^{F}BIAN led to the formation of the same [Co(^{F}BIAN)$_3$] with improved yield. Both complexes are sensitive towards oxygen and water. Strict anaerobic conditions should be applied during working with the extremely sensitive [Co(^{F}BIAN)$_3$].

[Ni^{II}(^{F}BIAN)$_2$] shows sharp signals in ^{1}H and ^{19}F NMR spectra demonstrating its diamagnetism, whereas **4** is clearly paramagnetic. The μ_{eff} measured for solid **4** at room temperature is found to be 3.80 μ_B, which is consistent with three unpaired electrons per molecular unit and spin state $S = 3/2$. By means of NMR and X-band EPR spectroscopy we did not detect any equilibrium between **3** and free ^{F}BIAN with a hypothetical octahedral nickel analogue of **4**. Complex **3** was EPR silent in solution/frozen solution in the temperature range 4–300 K.

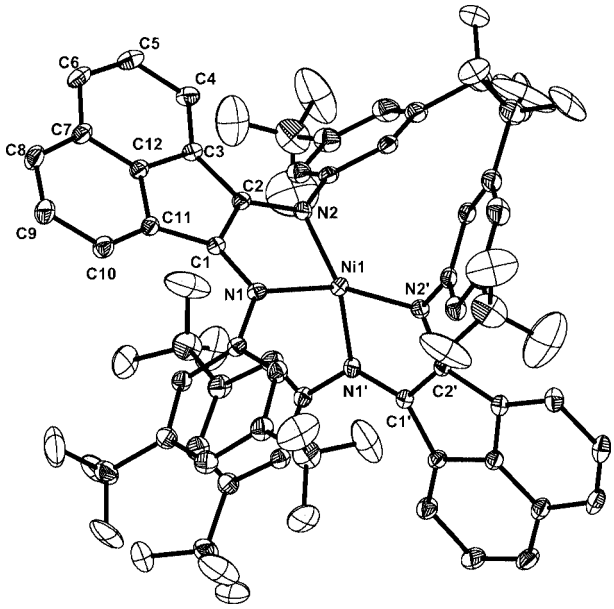

Figure 3. Molecular structure of **3**: disordered fluorine atoms are shown as semitransparent ellipsoids, hydrogen atoms are omitted for clarity, thermal ellipsoids are drawn at 30% probability level.

Crystal Structures of BIAN Complexes

The molecular structure of **3** consists of two planar chelating ^{F}BIAN ligands attached to the nickel atom (Figure 3). Similar to **1** and **2** the two ^{F}BIAN ligands in **3** form a distorted tetrahedral NiN_4 ligand environment. The dihedral angle formed by two diimine chelates is found to be 83.66(8)°.

It is interesting to note that the two almost orthogonal diimine ligands do not form a regular tetrahedron. Instead, one ligand seems to be turned around the axis through Ni, perpendicular to the plane of the other diimine. For visualization of this unusual geometry the first coordination sphere of **3** is depicted in Figure 4. Consequently, local symmetry is missing completely in **3**. In contrast, complexes **1**, **2**, and all structurally characterized [Ni(DAD)$_2$] complexes with diverse sterically demanding *N*-substituents,[8,9] as well as [Ca(dip-BIAN)$_2$] with bulky *N*-dip groups[17] all form distorted tetrahedra with pseudo C_2/D_2 symmetry. The distorted tetrahedral geometry of **3** can be ascribed to intermolecular arene–arene interactions observed in the crystal structure. The acenaphthene rings involved in π stacking are parallel with respect to each other and show an interplanar distance of 3.533 Å (see Figure S1 in the supporting information).

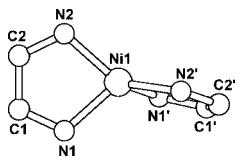

Figure 4. Ligands arrangement in **3**: a view exactly perpendicular to the plane defined by Ni1N1C1C2N2 (paper plane).

Oxidation state of the ligands can be unambiguously assigned by a bond lengths analysis. Typical bond lengths of bis(arylimino)acenaphthene ligand in different oxidation states are represented in Scheme 2. As the naphthalene system does not show distinct changes in bond lengths only C–N and C–C bond lengths of diimine moieties are given for the ligand in different oxidation states. In complex **3** the diimine C–N bond length is found to be on average 1.339(2) Å and the diimine bridging C–C bond is 1.427(3) Å long. After having compared the bond length pattern observed in **3** with those of known structures we assign both diimines in **3** to be in monoanionic radical form (Scheme 2). This implies that the oxidation state of Ni is +II and the electronic configuration of the metal is d^8.

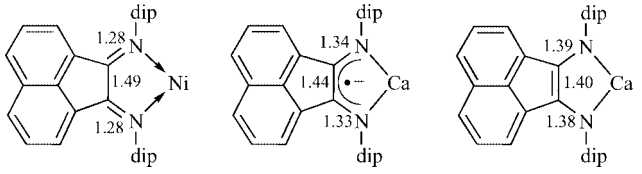

Scheme 2. Characteristic bond lengths for BIAN ligand in different oxidation states: $(BIAN)^0$ in $[Ni^{II}(dip\text{-}BIAN)Br_2]_2$[40] (left), $(BIAN)^{1-}$ in $[Ca^{II}(dip\text{-}BIAN)_2]$[17] (middle), and $(BIAN)^{2-}$ in $[Ca^{II}(dip\text{-}BIAN)(THF)_3]$[41] (right).

The *N*-phenyl rings in **3** form dihedral angles 57.9(1) and 49.9(1)° with the corresponding diimine moieties, hence the influence of these rings on the π system of ^{F}BIAN is negligible. The observed dihedral angles along with deviation of N–C(phenyl) bonds from the diimine planes can be readily ascribed to intramolecular interactions between sterically demanding substituted phenyl rings. The only structurally characterized complex of the type $[M(BIAN)_2]$ was reported very recently by Fedushkin et al.[17] The crystal structure of paramagnetic $[Ca^{II}(dip\text{-}BIAN)_2]$ reveals a dihedral angle of 28° between the diimine moieties and does not show any π stacking between the diimine moieties in the crystal lattice.

The molecular structure of cobalt complex **4** is represented in Figure 5. It consists of three(!) sterically demanding ^{F}BIAN ligands attached to the metal center. While complexes containing three less demanding DAD ligands are known,[25] to the best of our knowledge complexes containing three BIAN ligands are unknown so far.

The cobalt ion in **4** has a slightly distorted octahedral environment. Three diimine ligands show considerable planarity and planes of them are almost perpendicular to each other, as expected for a perfect octahedron. Taking into account that synthesis of complex **4** is performed under strong reducing conditions we disagree with its description as Co^{III} with three $(^FBIAN)^{1-}$ ligands. The oxidation state of the metal is assumed to be +II or lower. Analysis of bond lengths of diimines shows non-equivalence of the three ligands. Two ^{F}BIAN ligands are crystallographically identical (Table 1, form **I**), whereas the third one (form **II**) reveals a distinctly differing bond pattern. The bond length pattern observed in **II** closely resembles that in complex **3**. The diimine C–N bond on av. 1.331(3) Å and diimine C–C bond of 1.442(5) Å in **II** [1.339(2) and 1.427(3) Å, respectively, in complex **3**] are in agreement with the formulation of **II** as a radical monoanion. On the other hand, C–N bonds in **I** are significantly shorter, on av. 1.303(4) Å, the diimine C–C bond is significantly longer [1.474(4) Å] compared to **II** indicating neutral diimine character. Comparison of bond lengths in **I** with those of previously characterized complexes confirms that **I** is best described as neutral ligand. Hence complex **4** contains one diimine in form of the radical monoanion and two neutral diimine ligands. This implies that the oxidation state of the cobalt atom in **4** is best described as +I with d^8 electronic configuration and correct description of **4** is $[Co^I(^FBIAN)^0{}_2(^FBIAN)^{1-}]$.

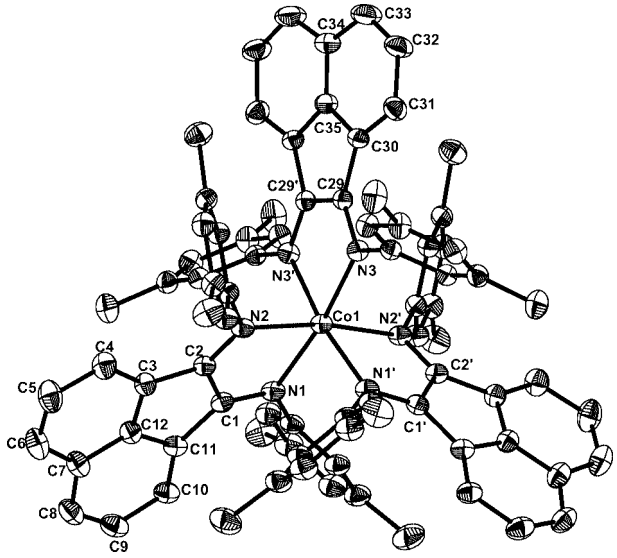

Figure 5. Molecular structure of **4**: hydrogen and disordered fluorine atoms are omitted for clarity, thermal ellipsoids are drawn at 30% probability level.

As expected the Co–N distances were found to be much longer in **4** compared to **2**. This is due to the increase of effective ionic radius $Co^{II}\rightarrow Co^I$ and to a change of coordination number from four in complex **2** to six in complex **4**. It can be noted that in complex **4** the distances Co–N in monoanionic $(^FBIAN)^{1-}$ at 2.125(2) Å are slightly shorter then those in closed-shell $(^FBIAN)^0$ at av. 2.132(2) Å. We refer this difference to the additional attraction between monoanionic $(^FBIAN)^{1-}$ and positive charged metal, which is lacking in the case of the neutral $(^FBIAN)^0$. The observed Co–N bond lengths are close to that reported for $[Co(bpy)_3]Cl$ at av. 2.11(2) Å.[26]

Magnetochemistry and EPR Spectroscopy

The electronic structures of the paramagnetic complexes **2** and **4** were further investigated by variable-temperature magnetic susceptibility measurements and X-band EPR spectroscopy.

The temperature dependence of the effective magnetic moment (μ_{eff}) of **2** is shown in Figure 6. The magnetic mo-

ment decreases gradually from 3.26 μ_B at 300 K to 2.36 μ_B at 5 K. From the crystal structure we have established that **2** contains Co^{II} ion (d^7) and two radical anionic ligands. Therefore **2** represents a three-center odd-electron system. The value of μ_{eff} at low temperatures is in agreement with a doublet ground state (S = 1/2). The first excited quartet state (S = 3/2) becomes populated with increasing temperature.

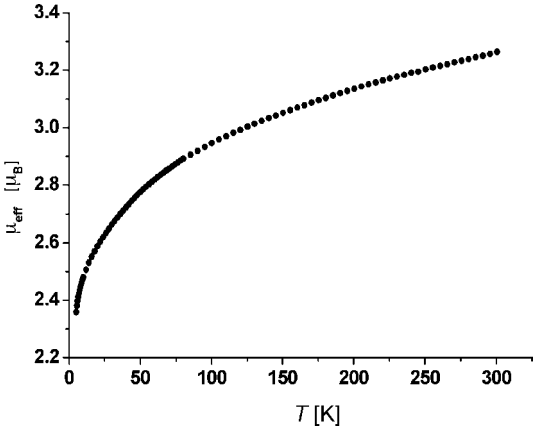

Figure 6. Temperature dependence of the effective magnetic moment of **2**.

The spin state of cobalt is not inherently clear because of the twisted coordination geometry around the metal center of **2**. Most cobalt(II) complexes are high-spin compounds (S_{Co} = 3/2) in tetrahedral, but low-spin (S_{Co} = 1/2) in planar environment. The molecular structure of **2** showing the dihedral angle of 58.0(2)° between the two diimines moieties takes an intermediate position between the tetrahedral and the planar geometries. The doublet ground state can be achieved by combination of the high-spin cobalt ion with the two radical ligands both coupled antiferromagnetically with the metal (Scheme 3, **A**). Another possibility to achieve the ground state doublet is to let the low-spin cobalt ion couple with two organic radicals, where two more types of electronic structures are to be considered. Two organic radicals couple in ferromagnetic fashion with each other but in antiferromagnetic fashion with the metal (**B**) yielding required S = 1/2. Or the two ligand spins couple antiferromagnetically with each other so that the metal spin is aligned ferromagnetically to one of the ligand spin but antiferromagnetically to the other one resulting in the doublet ground state (**C**).

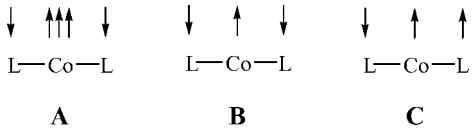

Scheme 3. Ground state spin models for **2**.

In recent publications by Wieghardt et al.[10] it was shown that related planar complexes $[M^{II}(sbqdi)_2]$ (M = Ni, Pd, Pt) containing radical ligands reveal strong antiferromagnetic coupling between two remote ligands. The ligands interact strongly with each other via an efficient superexchange mechanism that is mediated by a back-bonding interaction to the central metal. Such a superexchange interaction between two remote radicals is efficient only for certain geometries of the complexes. Very recently Ye et al.[27] showed, that if the geometry of such complexes deviates significantly from planarity, the interaction between two remote radical ligands becomes significantly weaker. Therefore, the spin state of **2** is likely to be of type **A** or **B**, with dominating antiferromagnetic interactions between the cobalt and radical ligand, but unlikely **C**, with dominating antiferromagnetic coupling between two radical ligands.

For fitting the experimental data we tentatively used the following Hamiltonian, see Equation (1).

$$\mathbf{H} = -J_{ab}(\mathbf{S_{Co}}\cdot\mathbf{S_1} + \mathbf{S_{Co}}\cdot\mathbf{S_2}) - J_{aa}(\mathbf{S_1}\cdot\mathbf{S_2}) + \beta[(\mathbf{S_1} + \mathbf{S_2})\cdot\mathbf{g_R} + \mathbf{S_{Co}}\cdot\mathbf{g_{Co}}]\cdot H \quad (1)$$

Here the first term is the Heisenberg term accounting for the isotropic exchange interaction between the metal and the radical ligands with J_{ab}, the second term relates to the isotropic exchange between two radical ligands with J_{aa}, and the third one is the Zeeman perturbation term. For the spin model **A** S_{Co} = 3/2 and for the model **B** S_{Co} = 1/2. The $\mathbf{g_{Co}}$ and $\mathbf{g_R}$ were assumed to be isotropic with g_{Co} and g_R principal values, for radical ligands $S_1 = S_2$ = 1/2. Unfortunately, we were not able to obtain a reasonable fit to the experimental data for both low- and high-spin cobalt complex models. The introduction of the intermolecular interactions and paramagnetic impurities did not improve the fit significantly. A more accurate model considering the local anisotropy and/or anisotropic interactions is therefore needed.

In spite of the unsuccessful simulations of magnetic susceptibility data, the ground state of **2** can be determined by EPR spectroscopy at cryogenic temperatures. Indeed, if we reject **C** because of geometrical reasons, then **A** and **B** would give apparently different EPR spectra at low temperatures. Model **A** would give the EPR signal typical for cobalt(II) complexes, whereas **B** would give a spectrum of an organic radical.

The X-band EPR spectrum of **2** measured in a frozen solution at 20 K is shown in Figure 7. The large anisotropy of the g tensor and the hyperfine splitting of ^{59}Co (I = 7/2) indicate that the unpaired electron is located mostly on the metal d-orbitals and not on the ligands. Therefore the model **A** with high-spin Co^{II} is the most plausible description of this system. The EPR spectrum of **2** has been successfully simulated by using the orthorhombic g tensor: g_1 = 4.296, g_2 = 1.676, g_3 = 1.625, with ^{59}Co hyperfine coupling constants: A_1 = 197, A_2 = 52, A_3 = 56 G. Furthermore, the line width dependence was introduced as shown in Equation (2), where m_I is the nuclear spin (m_I = –7/2, ..., +7/2 for ^{59}Co nucleus); α_i, β_i, γ_i are orientation-dependent ($i = x, y, z$) line width parameters.

$$\Delta B(m_I) = \sum_{i=1}^{3} \alpha_i + \beta_i m_I + \gamma_i m_I^2 \quad (2)$$

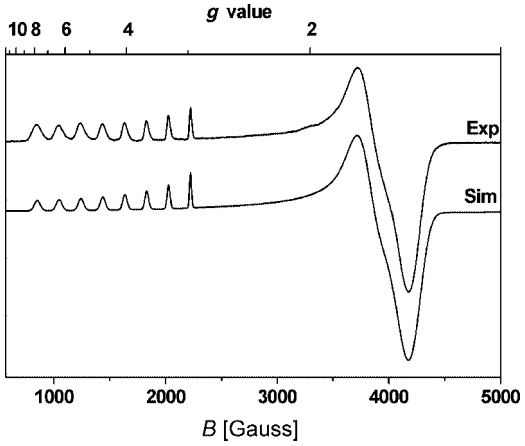

Figure 7. X-band EPR spectrum of **2**. Conditions: THF/toluene ca. 1:1 at 20 K; frequency 9.2265 GHz; power 5.0 μW; modulation amplitude 10 G. The fit parameters are given in the text.

The temperature dependence of μ_{eff} of **4** is shown in Figure 8. The magnetic moment measured at 300 K is 3.80 μ_B indicates the presence of three unpaired electrons (S = 3/2). With decreasing temperature μ_{eff} gradually decreases to the value of 2.07 μ_B at 10 K followed by a steep descent to 1.79 μ_B at 1.8 K. This behavior is explainable by the presence of the high-spin Co^I (d^8, S_{Co} = 1, pseudooctahedral environment) and a radical ligand (S_R = 1/2) coupled in antiferromagnetic fashion. Thus, the ground state of **4** is a doublet with an excited quartet populated at higher temperatures. The abrupt decreasing of the magnetic moment at temperatures below 10 K can be ascribed to the intermolecular antiferromagnetic interactions in the solid.

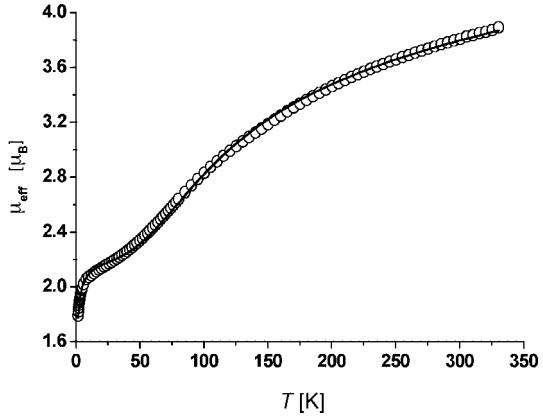

Figure 8. Temperature dependence of the effective magnetic moment of **4**, the fit parameters are given in the text.

To fit the experimental data we used the following Hamiltonian, see Equation (3), where the first term is the Heisenberg term related to the isotropic exchange interaction (J) between two magnetic centers and the second term is the Zeeman perturbation, nonequivalence of **g** tensors is supposed.

$$\mathbf{H} = -J\mathbf{S_{Co}}\cdot\mathbf{S_R} + \beta(\mathbf{S_{Co}}\cdot\mathbf{g_{Co}} + \mathbf{S_R}\cdot\mathbf{g_R})\cdot H \quad (3)$$

Assuming tensors $\mathbf{g_{Co}}$ and $\mathbf{g_R}$ to be isotropic with g_{Co} and g_R principal values and taking S_{Co} = 1, S_R = 1/2 the equation for magnetic susceptibility can then be derived, Equation (4).[28]

$$\chi = \frac{N\beta^2}{4kT}\frac{g_{1/2}^2 + 10g_{3/2}^2\exp(3J/2kT)}{1+2\exp(3J/2kT)} \quad (4)$$

Here $g_{1/2}$ and $g_{3/2}$ factors correspond to each of the spin states, they are related to the local g factors through Equation (5).

$$g_{1/2} = (4g_{Co} - g_R)/3 \qquad g_{3/2} = (2g_{Co} + g_R)/3 \quad (5)$$

By adding temperature-independent paramagnetism (*TIP*) into Equation (4) it was possible to obtain a good fit for magnetic susceptibility for the temperature range 10–330 K. To fit the data on the whole temperature range we modified Equation (4) according to the molecular field approximation for weak intermolecular interactions, Equation (6).[29] Here z is the number of the nearest neighbors around a given magnetic molecule in the crystal lattice and J' is the interaction parameter, the g factor in Equation (6) was taken as equal to 2.

$$\chi' = \frac{\chi}{1-(2zJ'/Ng^2\beta^2)\chi} + TIP \quad (6)$$

The best fit using Equation (6) was obtained with the following parameters: g_R = 2.00 (fixed), g_{Co} = 2.37, J = –106.0 cm^{-1}, zJ' = –0.78 cm^{-1}, $TIP = 1.23\times10^{-3}$ $cm^3\,mol^{-1}$. The accuracy of the fit used is very good showing R^2 = 0.99924. Hence, the ground state doublet is separated from the excited quartet by $-3J/2$ = 159 cm^{-1}. Week intermolecular antiferromagnetic interactions are present in the polycrystalline sample of **4**, as indicated by negative value of zJ' = –0.78 cm^{-1}. Abrupt decreasing of μ_{eff} of **4** at low temperatures may be governed by zero-field splitting effect as well, this supposition was not examined.

The X-band EPR spectrum of **4** measured in frozen solution at 4 K is shown in Figure 9. It is evident that more than one paramagnetic species is present. We propose two compounds to exist in the frozen solution. The first one is a cobalt complex with a large anisotropy of the g tensor (**Tet**): a well resolved octet centered at $g \approx 3.8$ and a less resolved signal at $g \approx 1.9$. The second species is a cobalt complex as well, but with a higher symmetric arrangement at the metal (**Oct**), its signal is partly hidden by those of **Tet** and centered at $g \approx 2.3$. Because **4** is extremely sensitive towards both oxygen and moisture, the EPR experiment was repeated several times with freshly prepared solutions. All samples measured gave nearly identical spectra. It was concluded that the two cobalt species observed originate not from decomposition of **4**, but from partially dissociation.

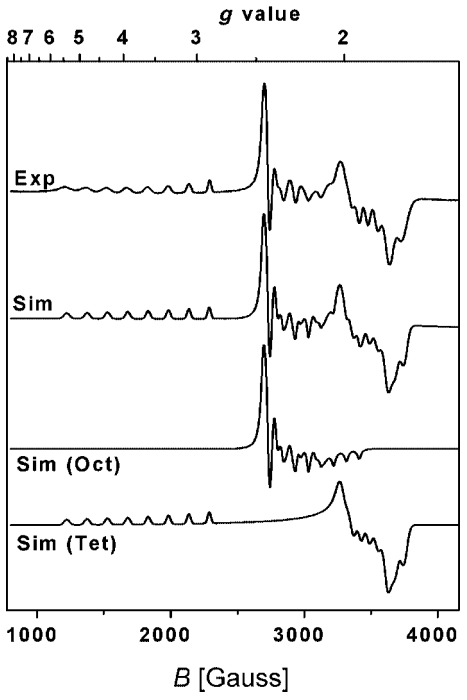

Figure 9. X-band EPR spectrum of **4**. Conditions: THF/toluene ca. 1:1 at 4 K; frequency 9.2278 GHz; power 1.3 μW; modulation amplitude 10 G. The fit parameters are given in the text.

Thus the distorted octahedral complex **4** partially dissociates in solution (toluene/THF ≈ 1:1) into the neutral species [Co(^{F}BIAN)$_2$], which has very likely distorted tetrahedral geometry, and the free ligand ^{F}BIAN. Assuming that this dissociation takes place we can readily assign the signals in the EPR spectrum. Species **Tet** is expected to be [Co(^{F}BIAN)$_2$], whereas **Oct** is apparently **4**. The EPR spectrum is therefore best explained by the superposition of two orthorhombic signals. The spectrum has been successfully simulated by using the following parameters: for **Oct** g_1 = 2.363, g_2 = 2.243, g_3 = 2.143, hyperfine coupling constants (^{59}Co) A_1 = 17, A_2 = 58, A_3 = 96 G; for **Tet** g_1 = 3.756, g_2 = 1.874, g_3 = 1.895, hyperfine structure (^{59}Co) A_1 = 153, A_2 = 65, A_3 = 38 G. For **Tet** showing the large anisotropy the line width dependence was included in the simulation. On warming, the signal of **Oct** disappears much faster than that of **Tet**. At 100 K only the poorly resolved signal of **Tet** is observed. This indicates that the relaxation time for **Oct** compared to **Tet** is small.

Electronic Spectra

Electronic spectra of the complexes **1**–**4** in chloroform and in *n*-hexane solutions were recorded at room temperature in the range 200–1100 nm. Spectra of DAD complexes **1** and **2** consist of a strong band in the ultra-violet ($\varepsilon > 10^4$ dm^3·mol^{-1}·cm^{-1}) and weaker two (**1**) or four bands (**2**) in the visible region. The UV absorption can be assigned to intra-ligand (IL) transition, since the free ligand absorbs in the similar region. The long-wavelength bands in visible, determining the intensive color of the complexes presumably are charge-transfer (CT) transitions. Solvent dependence and high intensity renders them easily distinguishable from solvent-independent and low-intensity d–d transitions. The two bands in the visible region are characteristic of [Ni(DAD)$_2$] complexes, as was observed by tom Dieck for a series of such complexes.[8]

UV/Vis spectra of BIAN complexes **3**–**4** are dominated by intense IL electronic transitions (329–332 nm, $\varepsilon > 10^4$ dm^3·mol^{-1}·cm^{-1}), and three transitions in visible/NIR. The latter are supposed to be CT transitions relying on their relative high intensities (ε = 8–10·10^3 and 5–12·10^3 dm^3·mol^{-1}·cm^{-1} for **3** and **4**, respectively) and solvatochromism. High-energy absorption maxima in visible at 512 and 519 nm for **3** and **4**, respectively, are indicative of the presence of a radical anion (BIAN)$^{1-}$. Several complexes reported recently by Fedushkin[30] containing the radical (BIAN)$^{1-}$ all show absorption maximum/maxima in the region 420–530 nm.

We refrain from discussing the more specific assignment of electronic absorptions of **1**–**4** in visible/NIR as sufficient confidence may only be achieved in combination with high-quality excited-state TD-DFT calculations.

Conclusions

We have synthesized new complexes of nickel and cobalt containing the non-innocent highly π acidic diimine ligands ^{F}DAD and ^{F}BIAN with bulky fluorinated *N*-substituents. The oxidation states of the ligands and subsequently of the metals were determined by single-crystal X-ray analysis at low temperatures. The electronic structure of [Ni^{II}(^{F}DAD)$_2$] as well as electronic structures of [Ni(DAD)$_2$] complexes previously characterized by X-ray analysis were shown to be consistent with a divalent nickel d^8 ion and a pair of radical monoanionic ligands. The unique [Co^{I}(^{F}BIAN)$_3$] comprises a cobalt(I) ion, two neutral (^{F}BIAN)^0 ligands and one radical monoanion (^{F}BIAN)$^{1-}$. Both [Co^{II}(^{F}DAD)$_2$] and [Co^{I}(^{F}BIAN)$_3$] possess a doublet ground state with electron density located mostly in the metal d-orbitals as was concluded from magnetic susceptibility measurements and the X-band EPR spectroscopy.

Experimental Section

The ligand C_6F_5-DAD(Me) (= ^{F}DAD) can be prepared by a known procedure in low yield.[31] Here we describe an alternative method of its preparation with much higher yield (vide infra). Anhydrous metal salts $NiCl_2$·DME,[32] $NiBr_2$·DME[32] as well as [3,5-$(CF_3)_2$-C_6H_3]-BIAN[33] (= ^{F}BIAN) and C_8K[34] were prepared according to the known procedures. Anhydrous $CoCl_2$ was obtained by refluxing of $CoCl_2$·nH$_2$O with $SOCl_2$ for several hours followed by removing the volatiles under reduced pressure at 90 °C. Syntheses of all complexes were performed under a dry argon atmosphere using standard Schlenk techniques and dried solvents.

Physical Measurements: Mass spectra were obtained on a Finnigan MAT 95S mass spectrometer (70 eV, EI). IR spectra were obtained in Nujol mull using a Nicolet 510 FT-IR. UV/Vis spectra were measured on a Shimadzu UV-1601PC instrument in absolute

$CHCl_3$ and *n*-hexane at concentrations 10^{-4} to 10^{-5} M. NMR spectra were recorded at room temperature on a Bruker ARX 200 spectrometer at 200.13 MHz for ^1H and 188.29 MHz for ^{19}F. ^1H NMR spectra are referenced (in ppm) to residual proton signals of $CDCl_3$ (δ = 7.26 ppm) and C_6D_6 (δ = 7.15 ppm). ^{19}F NMR spectra were referenced to external standard $CFCl_3$. Abbreviations used are the following: s = singlet, d = doublet, t = triplet, pst = pseudo-triplet, m = multiplet. EPR spectra were recorded in the X-band on a Bruker System ESP 300. The magnetic susceptibility measurements were performed on a powder samples using a Quantum Design MPMS2 SQUID magnetometer with an applied field of 1 T. Experimental susceptibility data were corrected for the underlying diamagnetism using Pascal's constants.

X-ray Crystallographic Data Collection and Refinement of the Structures: Single crystals of **1**–**4** were coated with inert oil, picked up with a glass fiber and mounted in the nitrogen cold stream of the STOE IPDS2 (**1**, **3**, **4**) or STOE IPDS diffractometer (**2**). Intensity data were collected at 193 K using graphite-monochromated Mo-K_α radiation (λ = 0.17073 Å). Data collection was performed by hemisphere runs taking frames at 1.0° in ω. Final cell constants were obtained from a least-squares fit of a subset of several thousand strong reflections. Intensity data of **1** and **3** were corrected using indexed crystal faces, the data of **4** using the semiempirical correction routine MulScanAbs.[35] For **2** an absorption correction did not improve the quality of the data and was not applied. There was disordered solvent (toluene) present in the crystal structures of **1**, **2**, and **4**. In the crystal structures of **3** and **4** the CF_3 groups are disordered: two positions for each fluorine atom with different occupancies were found. All structures have been solved by the direct methods in SHELXS-97[36] (**1**, **3**, **4**) or SIR92[37] (**2**) and refined using the full-matrix least-squares refinement procedure of SHELXL97,[36] all non-hydrogen atoms anisotropically; H atoms have been located and isotropically refined (**1**, **3**) or have been placed at calculated positions and have been refined using a riding model with $U_{iso}(H) = 1.2U_{eq}(C)$ (**2**, **4**). Crystallographic data of the compounds are listed in Table 2.

CCDC-290299 to -290302 contain the complete crystallographic data for this paper. These data can be obtained free of charge from The Cambridge Crystallographic Data Centre via www.ccdc.cam.ac.uk/data_request/cif.

Synthesis of C_6F_5-DAD(Me) (1a): To 2,3,4,5,6-pentafluoroaniline (9.15 g, 0.050 mol) dissolved in dry MeOH (15 mL), 2,3-butanedione (3.2 mL, 0.038 mol), *p*-toluenesulfonic acid (ca. 0.2 g), and trimethyl orthoformate (10.0 mL, 0.097 mol) were added. After stirring for 1 day at room temperature the pale yellow precipitate was filtered, washed with cold MeOH and dried in vacuo. Yield: 5.19 g (50%). ^1H NMR (200.13 MHz, $CDCl_3$, 300 K): δ = 2.24 (t, J = 1.2 Hz, 6H, CH_3) ppm. ^{19}F NMR (188.29 MHz, $CDCl_3$, 300 K): δ = –151.3 (d, $^3J_{F,F}$ = 20 Hz, 4F, Ar_{ortho}), –161.3 (t, $^3J_{F,F}$ = 21 Hz, 2F, Ar_{para}), –162.9 (pst, $^3J_{F,F}$ = 20 Hz, 4F, Ar_{meta}) ppm.

Syntheses of Complexes. [Ni^{II}{C_6F_5-DAD(Me)}$_2$] (1): $NiBr_2$·DME (371 mg, 1.20 mmol), C_8K (341 mg, 2.52 mmol) and **1a** (1000 mg, 2.40 mmol) were placed in a Schlenk flask and THF (50 mL) was added. The reaction mixture was stirred overnight at room temperature. The mixture was filtered via Celite and THF was removed in vacuo giving a purple powder. The raw product was repeatedly extracted with boiling toluene (50 mL) from a glass frit until almost colorless solution. After the toluene extract was stored for a night at –30 °C, dark-purple crystals were collected by decantation of the solvent. The crystals were washed with cold *n*-hexane (2 × 5 mL) and dried in vacuo. Yield: 660 mg (62%). Single crystals of **1** suitable for X-ray crystallography were obtained from a THF/toluene mixture (1:2) by cooling. M.p. 200–203 °C. $C_{32}H_{12}F_{20}N_4Ni$ (891.13): calcd. C 43.13, H 1.36, N 6.29; found C 43.66, H 1.85, N 5.96. MS (EI): *m/z* = 889 [M–H$^+$], 474 [M–(DAD)$^+$], 416 [(DAD)$^+$]. ^1H NMR (200.13 MHz, $CDCl_3$, 300 K): δ = –1.98 ppm (s, 12H, CH_3) ppm. ^{19}F NMR (188.29 MHz, $CDCl_3$, 300 K): δ = –150.2 (m, 8F, Ar_{ortho}), –160.1 (t, $^3J_{F,F}$ = 21 Hz, 4F, Ar_{para}), –164.0 (m, 8F, Ar_{meta}) ppm. IR (Nujol): $\tilde{\nu}$ = 1630 (w), 1508 (s), 1408 (s), 1308 (w), 1260 (w), 1196 (m), 1146 (w), 1117 (m), 1033 (s), 987 (s), 928 (m), 798 (w), 732 (m), 696 (w), 644 (w), 598 (w), 558 (w), 466

Table 2. Crystallographic data for **1**·(C_7H_8), **2**·(C_7H_8), **3**, and **4**·2(C_7H_8).

	1·(C_7H_8)	**2**·(C_7H_8)	**3**	**4**·2(C_7H_8)
Empirical formula	$C_{39}H_{20}F_{20}N_4Ni$	$C_{39}H_{20}CoF_{20}N_4$	$C_{56}H_{24}F_{24}N_4Ni$	$C_{98}H_{52}CoF_{36}N_6$
Formula mass [g/mol]	983.30	983.52	1267.50	2056.39
Crystal size [mm]	0.45 × 0.12 × 0.06	0.28 × 0.06 × 0.04	0.28 × 0.27 × 0.05	0.40 × 0.14 × 0.04
Crystal shape	plate	needle	plate	prism
Crystal system	orthorhombic	orthorhombic	monoclinic	monoclinic
Space group	*Pbcn*	*Pbcn*	*C*2/*c*	*C*2/*c*
a [Å]	*a* = 20.0534(10)	20.077(2)	18.3645(19)	28.843(2)
b [Å]	*b* = 12.9233(7)	12.9232(14)	18.1763(14)	13.3691(9)
c [Å]	*c* = 14.2875(10)	14.3559(12)	16.7383(18)	23.2949(19)
β [°]			113.662(12)	101.695(6)
V [Å^3]	3702.7(4)	3724.8(6)	5119.1(9)	8796.3(11)
Z	4	4	4	4
$D_{calcd.}$ [g/cm^3]	1.764	1.754	1.645	1.553
μ [mm^{-1}]	0.663	0.599	0.511	0.325
$\theta_{min.}/\theta_{max.}$ [°]	1.87/26.24	1.87/26.26	1.65/26.01	1.44/26.20
$T_{max.}/T_{min.}$	0.95/0.80		0.97/0.87	0.95/0.91
Reflections collected	33387	28558	25039	62074
Reflections unique	3719	3744	4890	8806
Reflections observed	2536	1825	3355	4840
No. of parameters	328	312	544	790
R(*F*)	0.0315	0.0527	0.0330	0.0507
Rw (F^2)	0.0810	0.0916	0.0714	0.1139
S (GOF) on F^2	0.896	0.910	0.876	0.908
$\Delta\rho_{max}$ [e Å^3]/$\Delta\rho_{min}$ [e Å^3]	0.30/–0.19	0.27/–0.35	0.26/–0.25	0.52/–0.38

(w) cm^{-1}. UV/Vis ($CHCl_3$): λ_{max} (ε_{max}/$dm^3 \cdot mol^{-1} \cdot cm^{-1}$) = 756 sh (3200), 524 (8000), ≈ 292 (15200) nm.

[Co^{II}{C_6F_5-DAD(Me)}$_2$] (2): $CoCl_2$ (156 mg, 1.20 mmol), C_8K (341 mg, 2.52 mmol) and **1a** (1000 mg, 2.40 mmol) were placed in a Schlenk flask and THF (40 mL) was added. The reaction mixture was stirred overnight at room temperature. The mixture was filtered and THF was removed in vacuo giving a brown powder. The raw product was extracted with *n*-hexane (65 mL), concentrated in vacuo and washed with cold benzene (5 mL). Yield: 431 mg (40%). Brown single crystals of **2** suitable for X-ray crystallography were obtained from a THF/toluene mixture (3:1) by cooling. M.p. 194–196 °C. $C_{32}H_{12}CoF_{20}N_4$ (891.38): calcd. C 43.12, H 1.36, N 6.29; found C 42.92, H 1.69, N 5.91. MS (EI): *m*/*z* = 890 [M–H^+], 475 [M–(DAD)$^+$], 416 [(DAD)$^+$]. IR (Nujol): $\tilde{\nu}$ = 1632 (w), 1514 (s), 1504 (s), 1402 (m), 1308 (w), 1197 (m), 1142 (w), 1119 (m), 1030 (s), 987 (s), 929 (m), 797 (w), 683 (m), 640 (w), 597 (w) cm^{-1}. UV/Vis ($CHCl_3$): λ_{max} (ε_{max}/$dm^3 \cdot mol^{-1} \cdot cm^{-1}$) = 697 (1200), 529 (3100), 470 (5400), 429 (5200), 335 (11600) nm.

[Ni^{II}({3,5-$(CF_3)_2C_6H_3$}-BIAN)$_2$] (3): $NiCl_2$·DME (610 mg, 1.00 mmol), C_8K (143 mg, 1.06 mmol) and ^{F}BIAN (111 mg, 0.51 mmol) were placed in a Schlenk flask and THF (30 mL) was added. The reaction mixture was stirred overnight at room temperature. The resulting dark-blue suspension was concentrated under reduced pressure. The raw product was extracted with toluene (40 mL). After toluene was removed, a dark-blue fine crystalline material was obtained, which was washed with MeCN and dried in vacuo. Yield: 518 mg (81%). Single crystals of **3** suitable for X-ray crystallography were obtained from a saturated *n*-hexane solution by cooling. M.p. 321–323 °C. $C_{56}H_{24}F_{24}N_4Ni$ (1267.47): calcd. C 53.07, H 1.91, N 4.42; found C 52.53, H 2.01, N 4.41. MS (EI): *m*/*z* = 1266 [M^+], 1247 [M–F^+], 662 [M–(BIAN)$^+$]. ^{1}H NMR (200.13 MHz, C_6D_6, 300 K): δ = 8.98 (s, 4H, H_{Ph}), 7.97 (m, 4H, H_{Ph}, H_{naph}), 7.10 (d, $^3J_{H,H}$ = 7.2 Hz, 2H, H_{naph}), 6.41 (pst, $^3J_{H,H}$ = 7.7 Hz, 2H, H_{naph}) ppm. ^{19}F NMR (188.29 MHz, C_6D_6, 300 K): δ = –63.0 (s, 12F, CF_3) ppm. IR (Nujol): $\tilde{\nu}$ = 1776 (w), 1600 (m), 1510 (w), 1418 (w), 1275 (s), 1243 (w), 1127 (s), 1091 (s), 1014 (s), 974 (m), 884 (m), 850 (m), 812 (m), 761 (m), 700 (m), 678 (m), 544 (w), 496 (w) cm^{-1}. UV/Vis ($CHCl_3$): λ_{max} (ε_{max}/$dm^3 \cdot mol^{-1} \cdot cm^{-1}$) = 874 (8300), 600 (12200), 512 (10300), ≈ 332 (32700) nm.

[Co^{I}({[3,5-$(CF_3)_2C_6H_3$]-BIAN}$_3$] (4): $CoCl_2$ (43 mg, 0.33 mmol), C_8K (95 mg, 0.70 mmol) and ^{F}BIAN (604 mg, 1.00 mmol) were placed in a Schlenk flask and THF (15 mL) was added. The reaction mixture was stirred overnight at room temperature. THF was removed in vacuo and the raw product was extracted with toluene (50 mL). Toluene solution was concentrated to 25 mL, *n*-hexane (25 mL) was added and the resulting solution was stored for a night at –30 °C. Solution was decanted, dark-purple crystals were washed with *n*-hexane and dried in vacuo. Yield: 283 mg (46%). Single crystals of **4** suitable for X-ray crystallography were obtained from a toluene/*n*-hexane mixture by cooling. M.p. 275–278 °C. $C_{84}H_{36}CoF_{36}N_6$ (1872.13): calcd. C 53.89, H 1.94, N 4.49; found C 53.44, H 1.96, N 4.47. MS (EI): *m*/*z* = 1267 [M–(BIAN)$^+$], 1248 [M–(BIAN)–F^+], 663 [M–2(BIAN)$^+$]. IR (Nujol): $\tilde{\nu}$ = 1600 (w), 1278 (s), 1261 (m), 1242 (m), 1175 (s), 1140 (s), 1102 (m), 1035 (m), 1019 (m), 972 (m), 892 (m), 856 (m), 846 (m), 822 (w), 795 (w), 770 (m), 723 (m), 705 (w), 683 (m), 668 (m), 616 (w), 576 (w), 533 (m), 513 (m), 481 (m) cm^{-1}. UV/Vis ($CHCl_3$): λ_{max} (ε_{max}/$dm^3 \cdot mol^{-1} \cdot cm^{-1}$) = 735 (5000), 519 sh (12100), ≈ 329 (41300) nm.

Supporting Information (see also the footnote on the first page of this article): Intermolecular π stacking in the crystal structure of **3** (Figure S1).

[1] A. L. Balch, R. H. Holm, *J. Am. Chem. Soc.* **1966**, *88*, 5201–5209.

[2] a) M. D. Ward, J. A. McCleverty, *J. Chem. Soc., Dalton Trans.* **2002**, 275–288; b) A. Vlček, Jr., *Coord. Chem. Rev.* **2002**, *230*, 225–242; c) P. Chaudhuri, K. Wieghardt, *Prog. Inorg. Chem.* **2001**, *50*, 151–216.

[3] H. tom Dieck, H. Bruder, *J. Chem. Soc., Chem. Commun.* **1977**, 24–25.

[4] H. tom Dieck, M. Svoboda, J. Kopf, *Z. Naturforsch. B: Chem. Sci.* **1978**, *33*, 1381–1385.

[5] D. von Walther, G. Kreisel, R. Kirmse, *Z. Anorg. Allg. Chem.* **1982**, *487*, 149–160.

[6] R. Kirmse, J. Stach, D. von Walther, R. Boettcher, *Z. Chem.* **1980**, *29*, 224–225.

[7] D. von Walther, *Z. Anorg. Allg. Chem.* **1974**, *405*, 8–18.

[8] a) M. Svoboda, H. tom Dieck, *Z. Naturforsch. B: Chem. Sci.* **1981**, *36*, 814–822; b) H. tom Dieck, M. Svoboda, T. Greiser, *Z. Naturforsch. B: Chem. Sci.* **1981**, *36*, 823–832.

[9] a) H. Görls, D. Walther, J. Sieler, *Cryst. Res. and Technol.* **1987**, *22*, 1145–1151; b) W. Bonrath, K. R. Pörschke, R. Mynott, C. Krüger, *Z. Naturforsch. B: Chem. Sci.* **1990**, *45*, 1647–1650.

[10] a) D. Herebian, E. Bothe, F. Neese, T. Weyhermüller, K. Wieghardt, *J. Am. Chem. Soc.* **2003**, *125*, 9116–9128; b) D. Herebian, K. E. Wieghardt, F. Neese, *J. Am. Chem. Soc.* **2003**, *125*, 10997–11005; c) V. Bachler, G. Olbrich, F. Neese, K. Wieghardt, *Inorg. Chem.* **2002**, *41*, 4179–4193.

[11] a) S.-M. Peng, Y. Wang, C.-K. Chiang, *Acta Crystallogr., Sect. C: Cryst. Struct. Commun.* **1984**, *40*, 1541–1542; b) C.-S. Lee, T.-S. Hwang, Y. Wang, S.-M. Peng, C.-S. Hwang, *J. Phys. Chem.* **1996**, *100*, 2934–2941.

[12] L. S. Hegedus, *Transition Metals in the Synthesis of Complex Organic Molecules*; University Science Books: Mill Valley, CA, **1994**, p. 3.

[13] C. K. Jörgensen, *Oxidation Numbers and Oxidation States*, Springer: Heidelberg, Germany, **1969**.

[14] P. Chaudhuri, C. N. Verani, E. Bill, E. Bothe, T. Weyhermüller, K. Wieghardt, *J. Am. Chem. Soc.* **2001**, *123*, 2213–2223.

[15] M. M. Khusniyarov, K. Harms, J. Sundermeyer, *J. Fluorine Chem.* **2006**, *127*, 200–204.

[16] a) R. van Asselt, C. J. Elsevier, W. J. J. Smeets, A. L. Spek, R. Benedix, *Recl. Trav. Chim. Pays-Bas* **1994**, *113*, 88–98; b) R. van Asselt, C. J. Elsevier, C. Amatore, A. Jutand, *Organometallics* **1997**, *16*, 317–328; c) L. K. Johnson, C. M. Killian, M. Brookhart, *J. Am. Chem. Soc.* **1995**, *117*, 6414–6415; d) C. M. Killian, D. J. Tempel, L. K. Johnson, M. Brookhart, *J. Am. Chem. Soc.* **1996**, *118*, 11664–11665.

[17] I. L. Fedushkin, A. A. Skatova, V. A. Chudakova, V. K. Cherkasov, S. Dechert, H. Schumann, *Russ. Chem. Bull. Int. Ed.* **2004**, *53*, 2142–2147.

[18] S. Blanchard, F. Neese, E. Bothe, E. Bill, T. Weyhermüller, K. Wieghardt, *Inorg. Chem.* **2005**, *44*, 3636–3656.

[19] a) L. R. Chamberlain, L. D. Durfee, P. E. Fanwick, L. M. Kobriger, S. L. Latesky, A. K. McMullen, B. D. Steffey, I. P. Rothwell, K. Folting, J. C. Huffman, *J. Am. Chem. Soc.* **1987**, *109*, 6068–6076; b) S. L. Latesky, A. K. McMullen, G. P. Niccolai, I. P. Rothwell, J. C. Huffman, *Organometallics* **1985**, *4*, 1896–1898; c) W. A. Herrmann, M. Denk, W. Scherer, F.-R. Klingan, *J. Organomet. Chem.* **1993**, *444*, C21–C24; d) K. Mashima, Y. Matsuo, K. Tani, *Organometallics* **1999**, *18*, 1471–1481; e) R. L. Huff, S.-Y. S. Wang, K. A. Abboud, J. M. Boncella, *Organometallics* **1997**, *16*, 1779–1785; f) K. Mashima, Y. Matsuo, K. Tani, *Chem. Lett.* **1997**, 767–768; g) T.-G. Ong, D. Wood, G. P. A. Yap, D. S. Richeson, *Organometallics* **2002**, *21*, 1–3; h) Y. Matsuo, K. Mashima, K. Tani, *Angew. Chem. Int. Ed.* **2001**, *40*, 960–962; i) J. Scholz, M. Dlikan, D. Strohl, A. Dietrich, H. Schumann, K.-H. Thiele, *Chem. Ber.* **1990**, *123*, 2279–2285; j) J. Wunderle, J. Scholz, U. Baumeister, H. Hartung, *Z. Kristallogr.* **1996**, *211*, 423–424; k) G. A. Hadi, J. Wunderle, K.-H. Thiele, R. Froehlich, *Z. Kristallogr.* **1994**, *209*, 372;

l) B. Richter, J. Scholz, J. Sieler, K.-H. Thiele, *Angew. Chem. Int. Ed. Engl.* **1995**, *34*, 2649–2651; m) A. Merkoulov, K. Harms, J. Sundermeyer, *Z. Anorg. Allg. Chem.* **2005**, *631*, 2877–2880.
[20] M. G. Gardiner, G. R. Hanson, M. J. Henderson, F. C. Lee, C. L. Raston, *Inorg. Chem.* **1994**, *33*, 2456–2461.
[21] a) G. S. Hall, R. H. Soderberg, *Inorg. Chem.* **1968**, *7*, 2300–2303; b) A. V. Reshetnikov, A. A. Sidorov, S. S. Talismanov, G. G. Aleksandrov, Y. A. Ustynyuk, S. E. Nefedov, I. L. Eremenko, I. I. Moiseev, *Russ. Chem. Bull. (Translation Izv. Akad. Nauk SSSR, Ser. Khim.)* **2000**, *49*, 1771–1774; c) H.-Y. Cheng, C.-C. Lin, B.-C. Tzeng, S.-M. Peng, *J. Chin. Chem. Soc. (Taipei)* **1994**, *41*, 775–781.
[22] M. M. Khusniyarov, K. Harms, J. Sundermeyer, B. Sarkar, W. Kaim, J. van Slageren, J. Fiedler, manuscript in preparation.
[23] S. Lorenzo, G. R. Lewis, I. Dance, *New J. Chem.* **2000**, *24*, 295–304.
[24] M. P. Thornberry, C. Slebodnick, P. A. Deck, F. R. Fronczek, *Organometallics* **2000**, *19*, 5352–5369.
[25] a) M. J. Blandamer, J. Burgess, J. Fawcett, P. Guardado, C. D. Hubbard, S. Nuttall, L. J. S. Prouse, S. Radulovic, D. R. Russell, *Inorg. Chem.* **1992**, *31*, 1383–1389; b) P. J. Daff, M. Etienne, B. Donnadieu, S. Z. Knottenbelt, J. E. McGrady, *J. Am. Chem. Soc.* **2002**, *124*, 3818–3819; c) K.-H. Thiele, B. Richter, B. Neumuller, *Z. Anorg. Allg. Chem.* **1994**, *620*, 1627–1630; d) M. N. Bochkarev, A. A. Trifonov, F. G. N. Cloke, C. I. Dalby, P. T. Matsunaga, R. A. Anderson, H. Schumann, J. Loebel, H. Hemling, *J. Organomet. Chem.* **1995**, *486*, 177–182; e) B. Chaudret, H. Koster, R. Poilblanc, *J. Chem. Soc., Chem. Commun.* **1981**, 266–268; f) B. Chaudret, C. Cayret, H. Koster, R. Poilblanc, *J. Chem. Soc., Dalton Trans.* **1983**, 941–945; g) B. Richter, J. Scholz, B. Neumuller, R. Weimann, H. Schumann, *Z. Anorg. Allg. Chem.* **1995**, *621*, 365–372.
[26] D. J. Szalda, C. Creutz, D. Mahajan, N. Sutin, *Inorg. Chem.* **1983**, *22*, 2372–2379.
[27] S. Ye, B. Sarkar, F. Lissner, T. Schleid, J. van Slageren, J. Fiedler, W. Kaim, *Angew. Chem. Int. Ed.* **2005**, *44*, 2103–2106.
[28] O. Kahn, *Molecular Magnetism*, VCH Publishers, New York, **1993**.
[29] C. J. O'Connor, *Prog. Inorg. Chem.* **1982**, *29*, 203–283.
[30] a) I. L. Fedushkin, A. A. Skatova, V. K. Cherkasov, V. A. Chudakova, S. Dechert, M. Hummert, H. Schumann, *Chem. Eur. J.* **2003**, *9*, 5778–5783; b) I. L. Fedushkin, A. A. Skatova, V. A. Chudakova, V. K. Cherkasov, G. K. Fukin, M. A. Lopatin, *Eur. J. Inorg. Chem.* **2004**, 388–393; c) I. L. Fedushkin, N. M. Khvoinova, A. Y. Baurin, G. K. Fukin, V. K. Cherkasov, M. P. Bubnov, *Inorg. Chem.* **2004**, *43*, 7807–7815; d) I. L. Fedushkin, A. A. Skatova, M. Hummert, H. Schumann, *Eur. J. Inorg. Chem.* **2005**, 1601–1608.
[31] J. C. Gordon, P. Shukla, A. H. Cowley, J. N. Jones, D. W. Keogh, B. L. Scott, *Chem. Commun.* **2002**, 2710–2711.
[32] L. G. L. Ward, D. M. Paul, *Inorg. Synth.* **1971**, *13*, 154–164.
[33] M. Gasperini, F. Ragaini, S. Cenini, *Organometallics* **2002**, *21*, 2950–2957.
[34] F. A. Cotton, E. A. Hillard, C. A. Murillo, X. Wang, *Inorg. Chem.* **2003**, *42*, 6063–6070.
[35] PLATON, A Multipurpose Crystallographic Tool, Utrecht University, Utrecht, The Netherlands, A. L. Spek, **2005**.
[36] SHELX97 – Programs for Crystal Structure Analysis (Release 97–2). G. M. Sheldrick, Institute of Inorganic Chemistry, University of Göttingen, Göttingen, Germany, **1998**.
[37] A. Altomare, G. Cascarano, C. Giacovazzo, A. Guagliardi, *J. Appl. Crystallogr.* **1993**, *26*, 343–350.
[38] T. Schleis, T. P. Spaniol, J. Okuda, J. Heinemann, R. Mülhaupt, *J. Organomet. Chem.* **1998**, *569*, 159–167.
[39] T. Spaniel, H. Görls, J. Scholz, *Angew. Chem. Int. Ed.* **1998**, *37*, 1862–1865.
[40] J. O. Liimatta, B. Lofgren, M. Miettinen, M. Ahlgren, M. Haukka, T. T. Pakkanen, *J. Polym. Sci., Part A: Polym. Chem.* **2001**, *39*, 1426–1434.
[41] I. L. Fedushkin, A. A. Skatova, V. A. Chudakova, G. K. Fukin, S. Dechert, H. Schumann, *Eur. J. Inorg. Chem.* **2003**, 3336–3346.

Received: March 15, 2006
Published Online: June 7, 2006

